Regulatory Mechanisms in Biosystems

ISSN 2519-8521 (Print)
ISSN 2520-2588 (Online)
Regul. Mech. Biosyst.

# Histological and physiological assessment of the effect of anti-inflammatory drug ketorolac trometamol on the heart and lungs of mice

A. I. Mohammed Salih*, M. N. Abed**, M. S. Musa*, A. K. Obayes*, M. S. J. Al-Ammash**

*University of Kirkuk, Kirkuk, Iraq
**University of Samarra, Samarra, Iraq

*Article info*
*Received 08.10.2025*
*Received in revised form 12.11.2025*
*Accepted 02.12.2025*

*Department of Biology, College of Education for Women, University of Kirkuk, Kirkuk, 36001, Iraq.*
*E-mail: ali-ibrahim@uokirkuk.edu.iq*

*Department of Religious Education and Islamic Studies, College of Islamic Sciences, University of Samarra, Samarra, 34010, Iraq.*
*E-mail: mymona.nagem.abed@gamil.com*

*Department of Biology, College of Education for Women, University of Kirkuk, Kirkuk, 36001, Iraq. E-mail: mohammed.s.musa@uokirkuk.edu.iq*

*Department of Biology, College of Education for Women, University of Kirkuk, Kirkuk, 36001, Iraq.*
*Tel.: +96-47-748-057-499.*
*E-mail: alikh@uokirkuk.edu.iq*

*Department of Pathological Analysis, Faculty of Applied Science, University of Samarra, Samarra, 34010, Iraq.*
*E-mail: ebnbaz87@gmail.com*

***Mohammed Salih, A. I., Abed, M. N., Musa, M. S., Obayes, A. K., & Al-Ammash, M. S. J. (2025). Histological and physiological assessment of the effect of anti-inflammatory drug ketorolac trometamol on the heart and lungs of mice. Regulatory Mechanisms in Biosystems, 16(4), e25214. doi:10.15421/0225214***

This study aimed to assess the influence of the nonsteroidal anti-inflammatory drug ketorolac on cardiotoxicity. Fifty albino mice were randomly divided into three equal groups: Group I, Group II, and Group III (single/daily intraperitoneal injection of 0.132, 0.66, and 1.32 mg/kg, respectively/for 12 days), and also the control group. After 48 h of treatment, blood samples were collected to evaluate cardiac enzymes, including troponin I, creatine kinase-MB, and myoglobin. The results showed, at the ultrastructural level, that the myocardium of Group I exhibited characteristic changes, including congested blood vessels, inflammatory cell infiltration between the muscle fibers, and dissociation of muscle cells. In Group II, karyorhexis atrophied. Group III showed necrosis of cardiomyocytes. We found a positive PAS reaction in the Purkinje fibers and cardiomyocytes and fibrosis in the heart muscle when compared with the control. Ultrastructurally, the lung of Group I revealed edematous and bronchiolar debris. Group II was observed to have necrosis of bronchioles and desquamation of alveolar cells. Group III showed hemosiderin deposition, and discontinuous and collapsed alveoli. We observed a PAS-positive reaction in the alveolar, bronchiolar, and pulmonary blood vessel walls; and also fibrosis of necrotic alveoli, bronchiolar, and blood vessel walls. The analysis of cardiac enzymes revealed a significant increase in troponin I in all experimental groups. On the other hand, a significant increase in myoglobin was seen in all experimental groups, whereas creatine kinase significantly increased in the groups II and III, $P < 0.05$ compared with the control group. In conclusion, this experimental study demonstrates for the first time the histopathological changes in the myocardial tissue and the lung, including congested blood vessels, atrophy, karyorhexis, and degeneration of myocardium, as well as inflammatory cell infiltration. In alveolar fibrosis, bronchial cellular debris was present. This reflects the toxicity of ketorolac during this experimental.

*Keywords*: ketorolac; cardiomyocytes; atrophy; lung; bronchiolar debris.

## Introduction

Nonsteroidal anti-inflammatory drugs (NSAIDs) are commonly used to mitigate pain during inflammatory responses (S et al., 2024). They are widely used due to their availability and affordability, which makes them a popular medication for pain management. While NSAIDs can be obtained without any prescription, medical staff often prescribe them in combination with other medications to reduce specific pain (Moro et al., 2016). These drugs exert analgesic, antipyretic, and anti-inflammatory effects and can be used for short-term postoperative, traumatic pain, and severe pain and swelling (Bosch et al., 2022). Nonsteroidal anti-inflammatory drugs can inhibit the enzyme cyclooxygenase (COX). This enzyme is required to convert cellular arachidonic acid into prostaglandins, prostacyclins, and thromboxanes (Shalabi et al., 2024). Their functions are fundamental to the body's internal environment. Thromboxanes play a major role in platelet adhesion, while prostaglandins act as vasodilators, contributing to reduced pain and fever (Gokul et al., 2023).

Ketorolac is a nonselective NSAID with a powerful analgesic effect (close to opioids) (Carneiro et al., 2014; Atefinezhad et al., 2022). The injectable formulation provides an immediate, effective analgesic therapy for the management of acute, severe pain, acting as an alternative to opioids for specific clinical situations (Lu et al., 2025). Ketorolac has a pharmacological and adverse effect identical to other NSAIDs (Forestell et al., 2023). Numerous clinical studies have used ketorolac for postoperative pain medication in children (Boric et al., 2017; Alsabri et al., 2025). Several studies have proposed the analgesic activity and safety of ketorolac (Esparza-Villalpando et al., 2024; Zhou et al., 2025) for post-surgery pain management (Uddin et al., 2008), particularly in dental surgery (Isiordia-Espinoza et al., 2022). It was found to be an effective analgesic for lumbar spinal cord surgery (Wang et al., 2022; Guan et al., 2024). Ketorolac is suitable as an intravenous dose in pediatric patients for headache analgesia (Lefchak et al., 2024).

The present study was carried out to assess the role of different dosages of ketorolac on the heart and lung tissues by evaluating the levels of cardiac enzymes (TnI, CK-MB, and myoglobin) in the serum of albino mice.

## Materials and methods

From March 2025 to May 2025, the entire experiment described in the present article was carried out in the animal house of Tikrit University's Veterinary Medicine College. The experiment involved forty male albino Swiss mice *Mus musculus* Balb/c, aged 8–9 weeks. The five mice were housed in plastic cages with a metal cover 13 * 16 * 30 cm, and they were fed commercial pellets and given water prior to the experiment. The mice were kept in suitable environmental conditions of 21–25 °C, with free access to food and water, and continuous cleaning cycles. The study was designed to investigate the effects of varying dosages of ketorolac trometamol 30 mg/mL (Oubari Pharma, Syria) on the heart and lung tissues, focusing on the levels of cardiac enzymes (TnI, CK-MB, and Myoglobin) in serum. The experimental animals were subdivided into three groups plus a control group. Group I received 0.132 mg/kg, Group II received 0.066 mg/kg, and Group III received 1.32 mg/kg of the drug daily for 12 days. The control group received saline 0.9 mg/L, injected intraperitoneally (Obayes et al., 2020). Biochemical tests: After 48 h of treatment and before euthanasia, blood samples were collected from 25 mice. The samples were then centrifuged to obtain serum to eva-

luate the levels of cardiac enzymes (TnI, Myoglobin Wondfo, Guangzhou Wondfo Biotech Co., Ltd. and CK-MB-Spin react, Spain Co.). Serum was collected and preserved at –20 °C for biochemical tests.

The remaining animals were kept until the end of the experiment and then euthanized by using a dosage inhalation of chloroform vapors inside a sealed glass container. Heart and lung samples from all experimental and control groups were fixed immediately with 10% neutral buffer formalin for 24 h. Fixed specimens were washed with tap water, ascending dehydrated ethyl alcohol, cleared in xylene, embedded in paraffin blocks at 60 °C, then sectioned by a microtome (7 μm thick) and stained with hematoxylin and eosin. Periodic acid–Schiff staining was used to detect glycogen and glycoprotein and polysaccharide, which appeared red. Masson's trichrome was used to visualize collagen, staining it blue. The tissue sections were mounted on the slides using Dibutylphthalate Polystyrene Xylene (DPX) and covered by cover slides (Obayes et al., 2020).

The data are expressed as mean ± standard deviation (SD). The differences were considered significant at p value below 0.05 using one-way ANOVA and post hoc Tukey test with Bonferroni correction.

## Results

The histological examination of the study's heart samples revealed a normal texture of intact cardiomyocytes in the control group. In Group I, the examination revealed complete blood hemolysis of congested blood vessels and inflammatory cells infiltrating underneath the pericardium. We observed dissociation of muscle fibers, perinuclear halo of cardiomyocytes, degeneration of cardiac muscle fibers, with inflammatory cell infiltration. Group II presented with karyorhexis of atrophied muscle fibers, with inflammatory cell infiltration between them; other muscle fibers exhibited a perinuclear halo of cardiomyocytes. The longitudinal section showed muscle fiber atrophy and a congested blood vessel. In Group III, we observed necrosis of muscle cells, with coarse infiltration by inflammatory cells and fibrocytes; on the other hand, the section showed karyorhex of muscle fibers and congested blood vessel (Fig. 1).

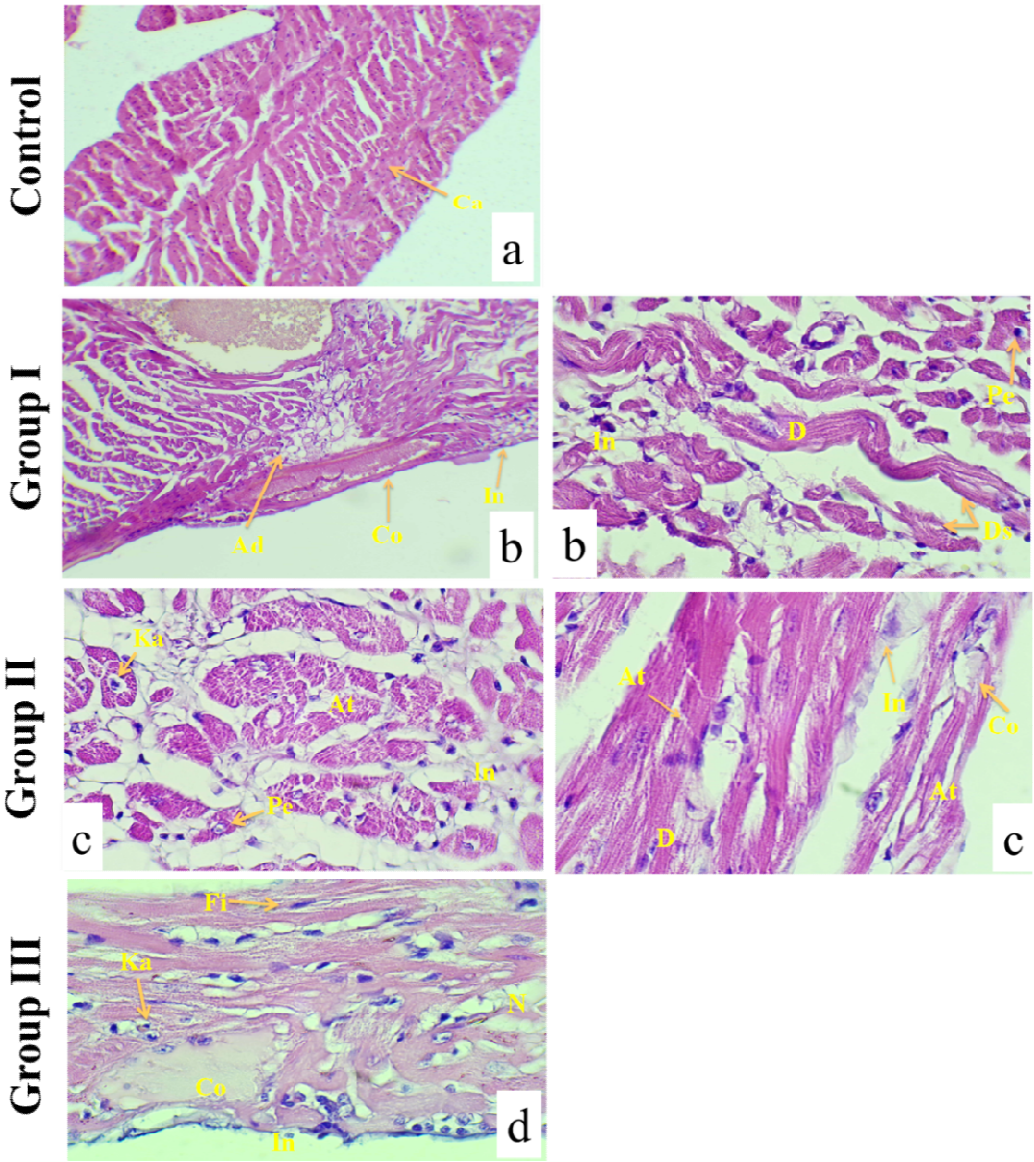


**Fig. 1.** Representative histological heart sections from mice stained with hematoxyline and eosin: *a* – control group demonstrating cardiomyocytes (Ca) ($10^x$); *b* – Group I showing complete blood hemolysis of congested blood vessels (Co), adipose tissue (Ad), and inflammatory cell infiltration (In) ($10^x$); *b* – Group I heart section with degeneration of muscles cells (D), inflammatory cell infiltration (In), dissociation of muscle fibers (Ds) and perinuclear halo of cardiomyocytes ($40^x$); *c* – Group II heart section with atrophy of muscle cells (At), inflammatory cell infiltration (In), karyorhex of muscle fibers (Ka) and perinuclear halo of cardiomyocytes (Pe) ($40^x$); *c* – Group II heart section with atrophy of muscle cells (At), inflammatory cell infiltration (In), longitudinal section showing atrophy of muscle fibers (At), and congested blood vessel (Co) ($40^x$); *d* – Group III heart section with necrosis of muscle cells (N), inflammatory cell infiltration (In), karyorhex of muscle fibers (Ka), and congested blood vessel (Co) ($40^x$)

The histological examination of the heart samples, stained with PAS (red), revealed that the control group had a negative reaction and had a normal texture of intact cardiomyocytes. In Group I, the heart sections revealed a positive reaction with pericardium, a sarcolemma of the Purkinje fibers, and pyknosis of degenerated cardiomyocytes. Dissociation of muscle fibers was observed. Group II showed blood vessels with luminal fibrinoid deposition and PAS-positive material, with tunics and adjacent cardiomyocytes, while the other cardiomyocytes underwent necrosis with the spread of inflammatory cells. Cardiomyocytes appeared with a high affinity for PAS-positive material, were undergoing necrosis, and were surrounded by inflammatory cells. Group III showed positive substances in the pericardium and Purkinje fibers with the degeneration of other muscle fibers. In addition to PAS-positive substances in the cardiomyocytes, they showed karyomegaly of the endocardium, with the spread of numerous inflammatory cells underneath it (Fig. 2).

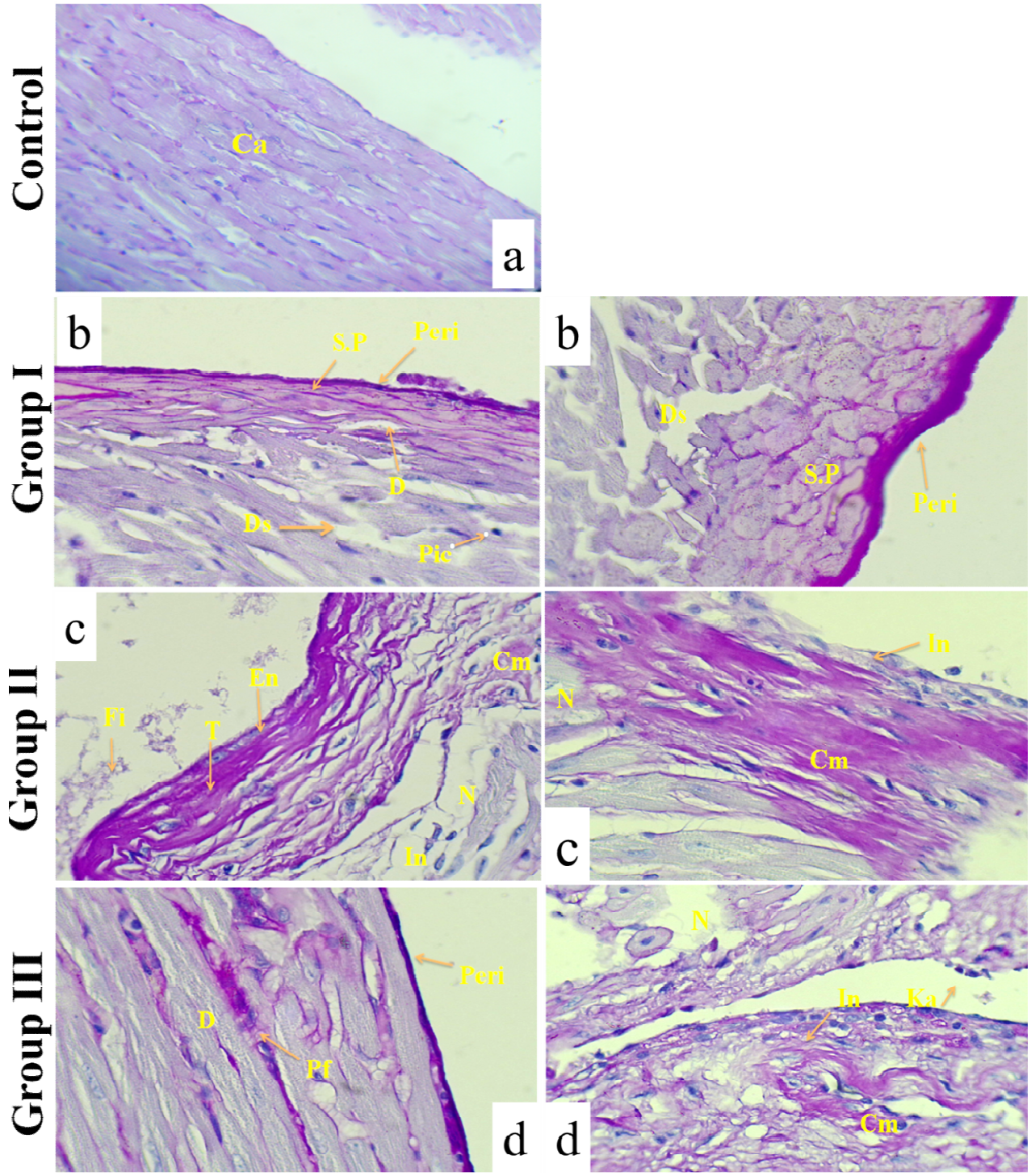


**Fig. 2.** Representative histological heart sections from mice stained with periodic acid-Schiff (PAS): *a* – control group heart section demonstrating PAS-negative reaction in cardiomyocytes Ca ($10^x$ PAS); *b* – Group I heart section with PAS-positive reaction in pericardium (Peri), sarcolemma of Purkinje fibers (S.P.), degeneration of cardiomyocytes (D), pyknosis of nucleus of muscle cells (Pic), dissociation of intercalated (discs in) between muscle fibers (Ds) ($40^x$ PAS); Group I heart section with PAS-positive reaction with pericardium (Peri), sarcolemma of cardiomyocytes (S), dissociation of intercalated discs between muscle fibers (Ds) ($10^x$ PAS); *c* – Group II showing PAS-positive reaction in endothelial layer (En), tunics of blood vessel (T) and adjacent cardiomyocytes (Cm), fibriniod deposition (Fi), necrosis of cardiomyocytes (N) and inflammatory cell infiltration In ($40^x$ PAS); *d* – Group III showing PAS-positive reaction in pericardium (Peri), Purkinje fibers (Pf), degeneration of cardiomyocytes (D), cardiomyocytes (Cm), necrosis of cardiomyocytes (N), karyomegaly of endocardium (Ka), and inflammatory cell infiltration (In) ($40^x$ PAS)

The histological examination of the heart samples, stained with Masson's trichrome to highlight collagen fibers (blue), revealed the following. Group I showed a spread of fibrosis and inflammatory cells between muscle bundles and adjacent blood vessels, loss of striations of cardiomyocytes, and atrophy of cardiomyocytes in some regions. Group II had a deposition of collagen fibers in the walls of the blood vessel and between the heart muscle fibers, and coarse inflammatory cell infiltration between muscle fibers. Other sections showed a spread of collagen fibers and neutrophils between necrotic muscle fibers and dissociation of atrophied muscle bundles. Group III was observed to have a coarse fibrosis between cardiomyocytes, with inflammatory cell infiltration. Other spots showed a spread of collagen fibers with inflammatory cells and fibroblasts between necrotic muscle fibers (Fig. 3).

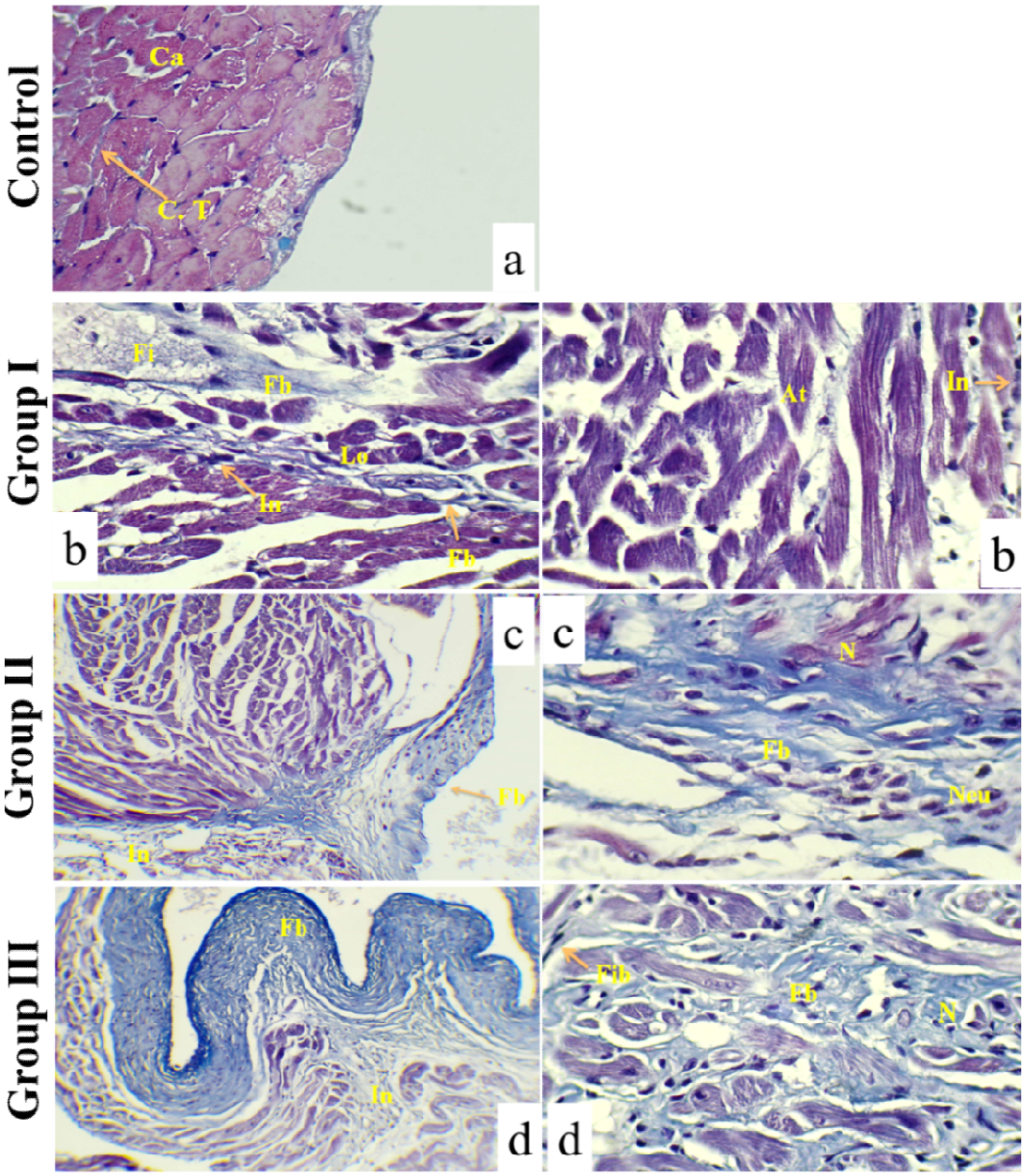


**Fig. 3.** Representative histological heart sections from mice stained with Masson's trichrome: *a* – control group demonstrating normal cardiomyocytes (Ca) and connective tissue of the heart (C.T.) (blue) ($40^x$); *b* – Group I showing fibrosis (Fb) and inflammatory cell infiltration (In) between cardiomyocytes and in adjacent blood vessel, loss of striations of cardiomyocytes (Lo), and atrophy of cardiomyocytes (At) ($40^x$); *c* – Group II showing fibrosis (Fb) and inflammatory cell infiltration (In) between cardiomyocytes and in adjacent blood vessel ($10^x$); heart section showing fibrosis (Fb) between necrotic (N) cardiomyocytes with infiltration by neutrophils (Neu) ($40^x$); *d* – Group III heart section with massive fibrosis (Fb) of cardiomyocytes with inflammatory cell infiltration (In) ($10^x$); heart section with fibrosis (Fb), inflammatory cell infiltration (In) and fibroblasts (Fib) between necrotic (N) cardiomyocytes ($40^x$)

The histological examination of the lung samples, stained with hematoxylin and eosin, revealed the following findings. The control group exhibited a normal texture of bronchioles, characterized by squamous epithelium types I and II. In Group I, the bronchiole underwent edematous changes. In addition, we observed a discontinuous, degenerated epithelial layer lining the bronchiole, with accumulation of cellular debris in its lumen. In the lung sections from Group II, we saw desquamation of alveolar cells, inflammatory cell infiltration of the plasma, and necrosis of bronchioles. Lung samples from Group III exhibited a massive inflammatory cell infiltration between congested blood vessels, with bubbles forming within them. Also, we observed an aggregation of cellular debris in the lumen of the bronchiole, with edematous tissue in the interstitial tissue. Other sections showed discontinuous degeneration of alveoli, collapse of alveoli, and congestion of hemolyzed blood vessels (Fig. 4).

The histological examination of the lung samples, stained with PAS (red) demonstrated the following. In the control group, the material was PAS-negative, with normal texture of the bronchioles' epithe-

lial layer, and PAS-negative in the alveoli, squamous epithelium type I and II. The material from Group I was PAS-positive, with both the sloughed epithelial layer and its degenerated lamina propria of bronchiole. Necrosis of alveoli was observed. Other section was PAS-positive, with cell debris in the lumen of bronchiole, degeneration of smooth muscle fibers, and damage to the basal lamina of degenerated alveoli. The interstitial space was filled with inflammatory cells. In Group II, the results were PAS-positive, showing accumulations of mucus, cellular debris in the lumen of bronchiole, and degenerated muscular layer, connective tissue of bronchioles, and lamina propria of necrotic alveoli, infiltrated by inflammatory cells. Another section was PAS-positive, with lamina propria of degenerated alveoli with edemas between the tissues. In Group III, the lung section was PAS-positive, with degenerated lamina propria of alveoli, and a massive hemorrhage within edematous interstitial tissue. We obtained PAS-positive material with tunics of congested blood vessel with fibriniod formation, and atrophy in adventitia (Fig. 5).

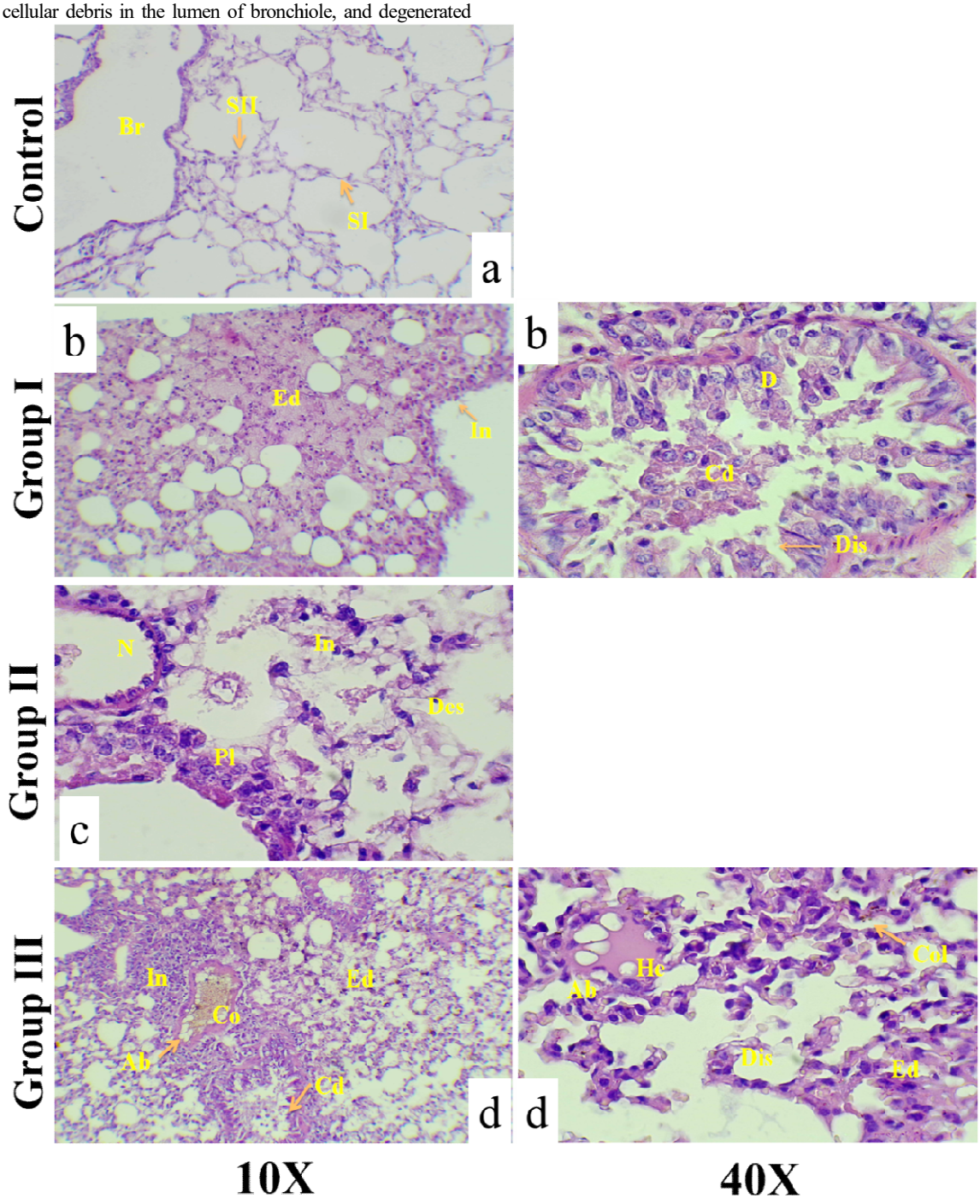


**Fig. 4.** Representative histological lung sections from mice stained with hematoxyline and eosin: *a* – control group showing normal texture of bronchioles (Br), squamous epithelium type I and II (SI, SII); *b* – Group I showing edema between air sacs (Ed) and inflammatory cell infiltration (In), bronchiole showing discontinuity of degenerated (D), epithelial layer (Dis), and aggregate of cellular debris (Cd); *c* – Group II showing discontinuity of desquamated alveoli (Des), infiltration of plasma, inflammatory cells (In), (Pl), necrosis in epithelial layer of bronchioles (N); *d* – Group III showing aggregate cellular debris in lumen of bronchiole (Cd), massive infiltration by inflammatory cells (In), edema between alveoli (Ed), and air bubble within congested blood vessel (Co), discontinuous edema between alveoli (Ed), collapsed alveoli (Col), and air bubble within hemolyzed congested blood vessel (He)

The histological examination of the lung samples, stained with Masson's trichrome for collagen fiber (blue), revealed normal interstitial tissue and alveoli in the control group. In Group I, we observed an increased deposition of collagen fibers in blood vessel tunics and a spread between necrotic alveoli and their lamina propria. Another section showed a deposition of collagen fibers in the wall of the bronchi-

ole. In Group II, we observed a high deposition of collagen fibers in the tunics of the blood vessel wall with fibrinoid deposition in its lumen. On the other hand, collagen fibers were spread out, with infiltration of inflammatory cells within the interstitial space, and in Group III, the whole section appeared fibrotic, with inflammatory cell infiltration. In addition, hemosiderin deposition within congested blood vessels was observed. Collagen fibers were deposited and spread in the interstitial tissue and within the wall of the blood vessel (Fig. 6). The analysis of cardiac enzymes revealed a significant ($P < 0.05$) increase in troponin I and myoglobin in all experimental groups compared with the control. Creatine kinase showed a significant ($P < 0.05$) increase in Group II and Group III, compared with Group I and the control group (Table 1). However, a nonsignificant differences existed beween Group I and Control.

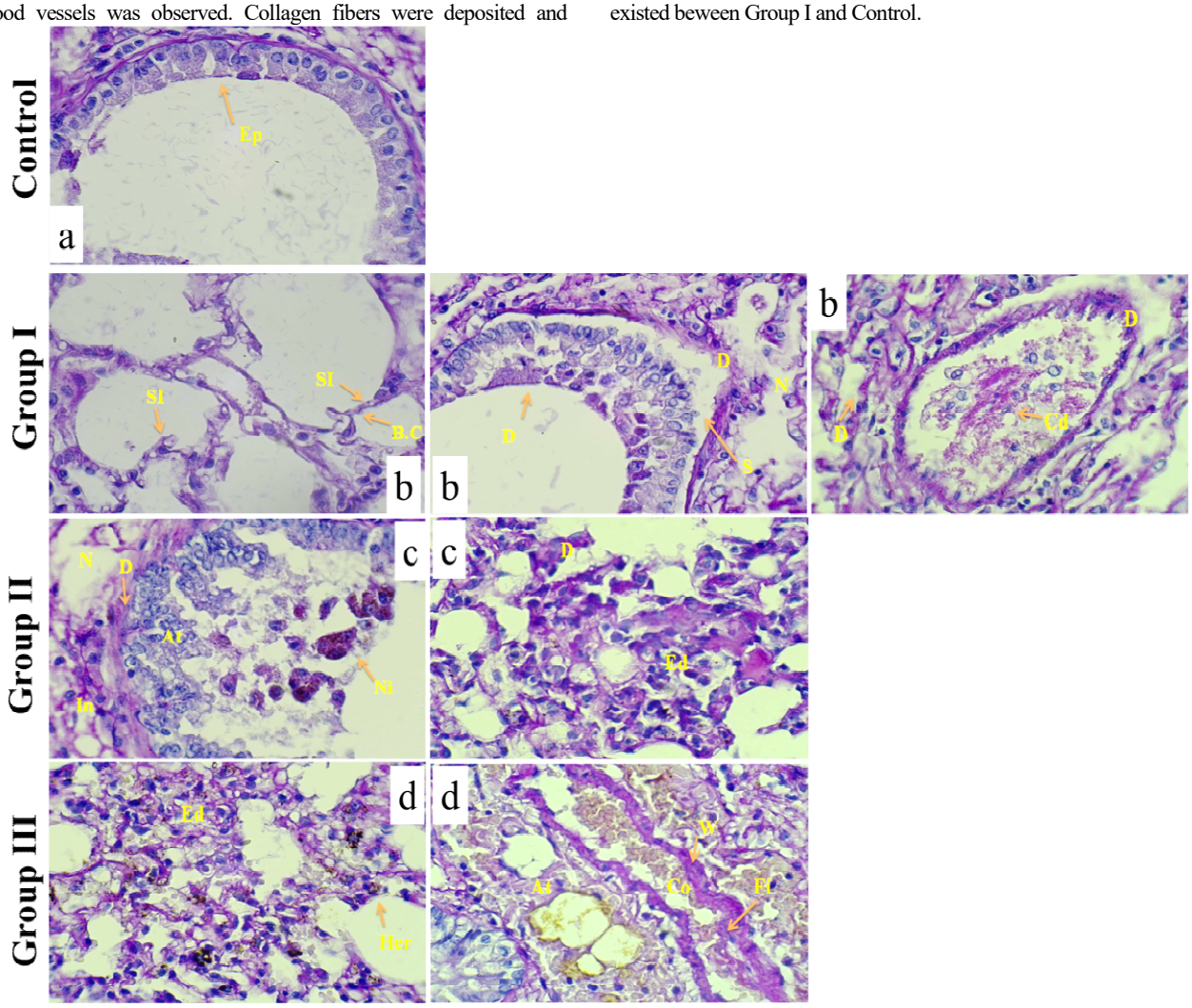


**Fig. 5.** Representative histological lung sections from mice stained with hematoxyline and eosin and periodic acid-Schiff (PAS) at 40$^x$ magnification: *a* – control group showing normal texture of bronchioles' epithelial layer Ep (PAS); control group showing normal texture of alveoli, squamous epithelium type I and II (SI, SII) and blood capillary B.C.; *b* – Group I showing PAS-positive reaction in accumulated mucus and separation of the bronchiole S, degeneration (C.T) necrosis of alveoli, spot accumulation of cell debris within lumen of bronchiole (S), degeneration of (C.T) alveoli with inflammatory cell infiltration (PAS); *c* – Group II showing PAS-positive reaction in accumulation of necrotic material within lumen of bronchiole (Ni), atrophy of epithelial line of bronchiole (At), degeneration of smooth muscle fibers and (C.T) layer of lamina propria of necrotic alveoli with inflammatory cell infiltration, lamina propria of degenerated alveoli with edema between alveoli (PAS); *d* – Group III showing PAS-positive reaction in degenerated alveoli with hemorrhage (Her) between alveoli, edema Ed, wall of congested blood vessel (W), with fibrin deposition (Fi), edema (Ed), and atrophy in adventitia (At) (PAS)

## Discussion

Nonsteroidal anti-inflammatory drugs (NSAIDs) are commonly used for mitigating pain and managing inflammatory responses (McDonald et al., 2018; S et al., 2024). Myocardial infarction induced by drugs refers to cardiomyocyte cell death caused by both illicit drugs and prescribed medications (Boarescu & Boarescu, 2024). These medications can induce myocardial infarction through several mechanisms, including coronary contraction, increased myocardial oxygen needed, endothelial degeneration, and direct toxic effects on the cardiomyocytes or atherosclerosis (Barachini et al., 2023; Mohammad et al., 2025).

In the present study, ketorolac was found to induce numerous histological alterations, including blood hemolysis in congested blood vessels. Akşit et al. showed that the increased intravenous pressure induced venous hypertension, triggering inflammatory cells, macrophage infiltration and hemosiderin accumulation in the myocardial tissue (Akşit et al., 2023). Nonsteroidal anti-inflammatory drugs are selective COX-2 inhibitors that inhibit vascular prostacyclin secretion (PGI2) (Tjenggal et al., 2021). Prostaglandin I2 (PGI2) acts as a vasodilator and has antiplatelet aggregation properties. This inhibition can be reduced by blocking COX-1, which causes vasoconstriction and is involved in thromboxane A2 production (Szczuko et al., 2021). Prostaglandin GI2 also inhibits the proliferation of smooth muscle cells and aggregates of white blood cells, thus inhibiting the formation of atherosclerosis (Katusic et al., 2012). Suppression of vital roles of COX reduced vascular dysfunction and infiltration of the aorta tunica by macrophages in mice treated with angiotensin II (Avendaño et al., 2016). The adverse effects of NSAIDs on the cardiovascular enzymes are related to blood pressure control and coagulation (das Dores Lopes et al., 2022).

**Table 1**
The heart enzymes in the control and experimental groups

| Parameters | Control | Group I | Group II | Group III |
|---|---|---|---|---|
| Troponin I, ng/mL | 0.1000 ± 0.001 D | 0.2140 ± 0.1673 C | 0.9060 ± 0.0002 B | 1.0360 ± 0.1128 A |
| Ck – MB, mg/dL | 2.140 ± 0.055 C | 2.920 ± 0.130 C | 12.940 ± 2.390 B | 17.000 ± 1.581 A |
| Myoglobin, ng/mL | 41.16 ± 0.85 D | 94.20 ± 2.49 C | 101.40 ± 6.11 B | 130.20 ± 11.97 A |

*Notes*. Data expressed as mean±SD, different letters indicate significant differences at P value less than 0.05 using one-way ANOVA and the post hoc Tukey test with Bonferroni correction.

In the our study, we observed a perinuclear halo of cardiomyocytes, degeneration in cardiac muscle fibers with inflammatory cell infiltration between them, karyorrhexis of atrophied muscle fibers, and necrosis of muscle cells of the heart. Lin et al. revealed the effects (histopathology) of arrhythmogenic drugs on cardiomyocytes, such as replacement of myocardium with inflammatory fibrofatty tissue; dissociation of muscle fibers, necrosis spread between otherwise intact cardiomyocytes, and multifocal inflammatory cell infiltration repeatedly seen in both heart ventricles (Lin et al., 2021). Diclofenac affects glutathione peroxidase enzyme levels, which protect cardiomyocytes against reactive oxygen species (ROS) in mice (Dolanbay et al., 2021). Reactive oxygen species lead to an imbalance by playing a major role in any pathological defect in the cardiovascular system, causing oxidative stress and inducing abnormal contraction and inflammatory cell proliferation (Koohsari et al., 2016), or lipid peroxidation during the pumping of the blood from the ischemic heart (Chen et al., 2018; Vupputuri et al., 2015). Cheng et al. declared that the reduction in levels of prostaglandin E2 by nonsteroidal anti-inflammatory drugs (NSAIDs) in patients usually influences the tissue repair mechanism in myocardial ischemia, which induces arrhythmias, microvascular dysfunction, and even muscle fiber necrosis (Cheng et al., 2021).

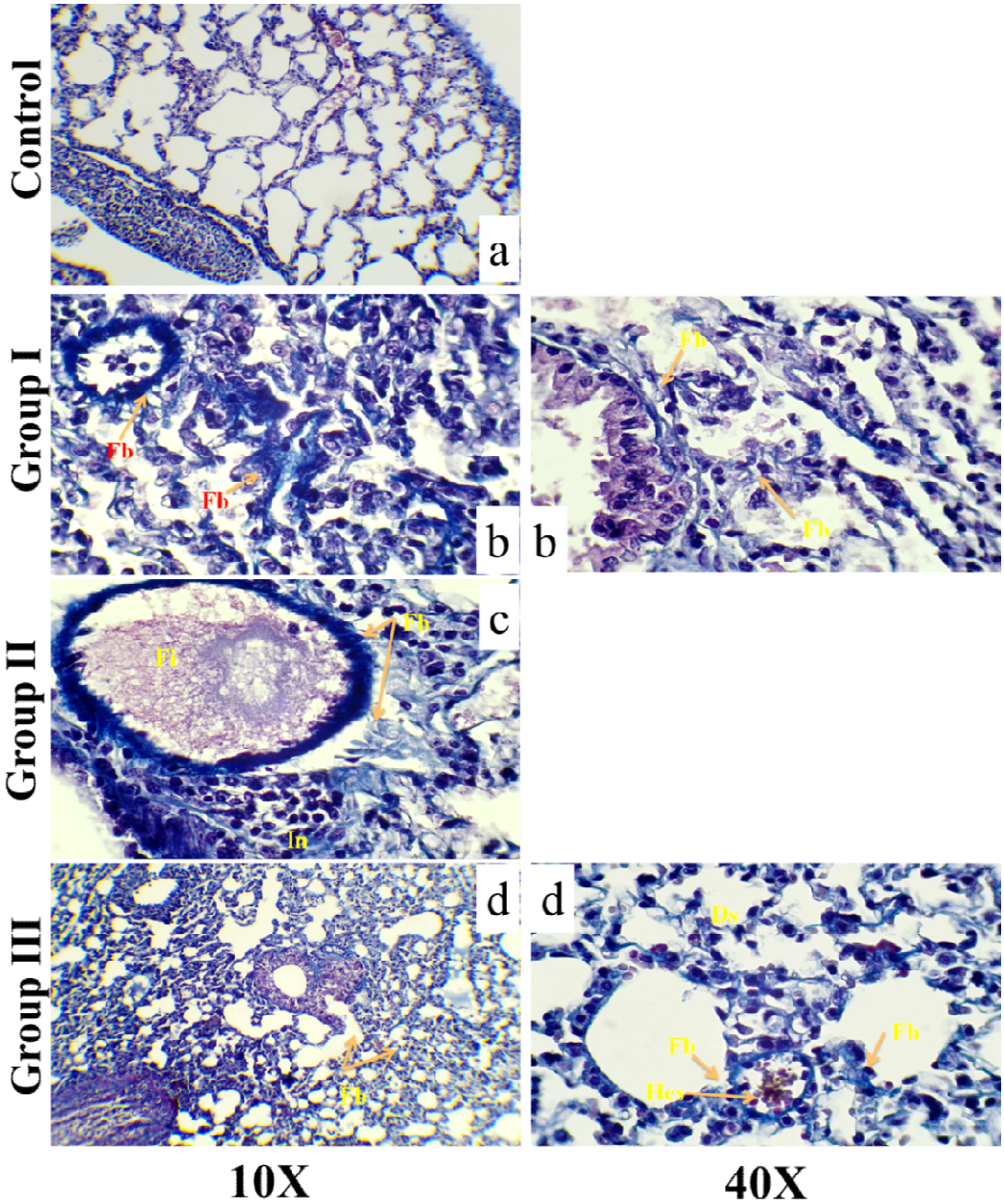


**Fig. 6.** Representative histological lung sections from mice stained with Masson's trichrome: *a* – control group showing normal interstitial tissue and alveoli; *b* – Group I showing fibrosis (Fb) around blood vessel wall, between alveoli, and around bronchioles' wall; *c* – Group II showing fibriniod deposition in lumen (Fi), fibrosis around blood vessel wall (Fb), and inflammatory cell infiltration (In); *d* – Group III showing fibrosis (Fb) in the whole section, inflammatory cell infiltration (In), fibrosis around congested blood vessel wall (Fb), with hemosiderin deposition (Hes), and fibrosis around collapsed alveoli (Ds)

In the present study of heart sections, the PAS revealed a high affinity for accumulation of glycogen in all experimental groups, such as pericardium and Purkinje fibers, a specialized type of cardiac muscle fiber that is responsible for the conduction of electrical impulses (Elbrønd et al., 2023). Milutinović et al. showed in their study that neurotoxin 3-nitropropionic acid induced a cardiomyopathy accompanied by the accumulation of glycogen granules in cardiac muscle fibers when compared with the control group (Milutinović & Zorc-Pleskovič, 2012). Cardiac glycogen decreases due to exposure to electromagnetic field (Zahkouk et al., 2015). Tejado et al. revealed an accumulation of glycolipids within the sarcoplasm, resulting in a vacuolated cytoplasmic appearance and fragmentation of myofibrillar filaments, ultimately leading to hypertrophy of cardiomyocytes (Tejado & Jou, 2018). Nguyen et al. (2009) revealed that PAS-positive material had cardiomyocytes, which may have a regulatory function in interstitial Cajal-like cells, cytoplasmic processes, pulmonary vessels, and atrial myocytes.

Staining the heart sections with Masson's trichrome showed a massive spread of collagen fibers (fibrosis) and inflammatory cells spreading in the walls of the blood vessels and between the heart muscle fibers. In patients with chronic atrial fibrillation, there was an inflammatory cell infiltration with a collagen fiber deposition (Tashiro et al., 2017). Fibroblast cells are the most predominant cell type in the heart, exhibiting proliferative activity in response to muscle cell injury. They interact with other cell types (Wang et al., 2022). A clinical study showed that ibuprofen, a member of NSAIDs, may increase the risk of irregular heartbeat and may even contribute to the increase in the incidence of sudden cardiac arrest (Pászti et al., 2021). Atrial fibrillation and hypertensive cardiomyopathy induce inflammation, dysfunction of coronary arteries, atrial fibrosis, hypertrophy of cardiomyocytes, and heart failure (Severino et al., 2021). The deficiency of Cox-2, regardless of Cox-1 deficiency, in adult rats induced myocardial fibrosis due to a reduction of cardiac ATP and acetyl-CoA production (Ricciotti et al., 2024). In the present study, fibrosis in all tunics of the cardiac blood vessel wall and cardiomyocytes was obvious. Myofibroblasts can progressively occupy the extracellular space between necrotic cardiomyocytes and the thickening of the vessel wall (Wang et al., 2022).

The lung is vitally remodeled in response to inflammation, and the gases are exchanged between alveoli and blood capillaries (Zhou et al., 2025). In the present study, we found edematous areas between the alveoli of the lung. During lung injury, PGF2 plays a major role in various functions, including inflammation and neutrophil migration in the lung tissue (Claar et al., 2015). During bleomycin-induced pulmonary fibrosis, the overproduction of free radicals (reactive oxygen species ROS)—due to the chelation of metal ions and reaction of the formed pseudoenzyme with oxygen—induced epithelial cell apoptosis (days 1–3), infiltration of inflammatory cells (days 3–9, neutrophils found in the bronchoalveolar lavage fluid at day 3 and lymphocytes at day 6), and fibroblasts activation, and produced extracellular matrix (days 10–21) (Tashiro et al., 2017). The same was seen in the present study: sections of bronchiole with accumulation of cellular debris and degeneration of alveolar walls.

The PAS-positive stain reaction demonstrates deposits in the bronchioles and alveoli (Liu et al., 2022), as the positive reaction stains carbohydrates of the tissue (glycogen, mucin) in alveoli and their basement membrane (Van-Seuningen & Davril, 1992). In the current study, we found a positive polysaccharide stain reaction associated with the accumulation of cell debris within the lumen of bronchioles, bronchiolar walls, and the lamina propria of necrotic alveoli as a side effect of the drug due to toxicity.

In our study, we also observed collagen fiber deposition (fibrosis) in blood vessel walls, compensating for the lamina propria of necrotic alveoli, and inflammatory cell infiltration. Increased vascular permeability plays a pathogenic role during extensive pulmonary inflammation and fibrosis (Probst et al., 2020). In recent years, researchers have shown that COX-2 exerts a protective effect against pulmonary fibrosis (Maher et al., 2010). Thus, inflammatory cell infiltration is a chronic inflammation process involved in a significant increase in numbers of macrophages, neutrophils, and lymphocytes (Miao et al., 2023). Obayes et al. (2024) demonstrated that diclofenac is a COX-2 inhibitor that blocks prostaglandin $E_2$ secretion, turning on activated myofibroblasts to induce pulmonary fibrosis. These inflammatory cells lead to differentiation of the lung fibroblasts into myofibroblasts, which are responsible for secreting collagen fibers into the alveolar interstitial tissue to induce pulmonary fibrosis (Bormann et al., 2021). One proposed mechanism of lung fibrosis in animal models involves bleomycin, which leads to apoptosis. The lung bleomycin hydrolase enzyme is retained at low levels in the lungs, thereby contributing to bleomycin-induced epithelial cell injury (Tashiro et al., 2017).

This study demonstrates a significant alteration in the levels of cardiac enzymes troponin I, CK-MB, and myoglobin. Troponin is an important biomarker of cardiac injury; and the cTnT level can persist in the patient's serum for up to 72 hours (Babuin & Jaffe, 2005). The CK-MB enzyme is associated with the measurement of the troponin in ischemic heart disease (Irmak et al., 2021). This alteration in enzyme levels, indicating degeneration, inflammation, atrophy, and fibrosis, was shown in the results of our study. The doxorubicin chemotherapy was observed to induce cardiomyopathy, accompanied by cytoplasmic membrane leakages and a high level of troponin (Sorodoc et al., 2022). The findings of this study align with those of Okwakpam et al., demonstrating that diclofenac induces leakage of both troponin I and LDH in serum, which is attributed to decreased glutathione levels and adverse effects on rats (Okwakpam et al., 2023).

## Conclusion

Ketorolac in this experimental animal model study induced numerous histological defects in the myocardium, such as congested blood vessels, degeneration in the cardiac muscle fibers, inflammatory cell infiltration, and karyorhexis of atrophied muscle fibers. In the lung, ketorolac induced alveolar fibrosis and bronchial inflammation, characterized by the presence of cellular debris. This reflects the toxicity of ketorolac during the experiment.

This research did not receive any specific grant from funding agencies in the public, commercial, or not-for-profit sectors.

The authors declare that they have no known competing financial interests or personal relationships that could have appeared to influence the work reported in this paper.

## References

Akşit, E., Büyük, B., & Oğuz, S. (2023). Histopathological changes in myocardial tissue due to coronary venous hypertension. Archives of Medical Science, 19(6), 1714–1720.

Obayes, A. K., Hameed, H. A., & Mohammedsalih, A. I. (2024). Histological investigation for the effect of non-steroidal anti-inflammatory drug [diclofenac] on myocardium and lung of local breed Rabbit. Open Access Research Journal of Life Sciences, 8(2), 46–54.

Alsabri, M. A. H., Diab, R. A., Alqeeq, B. F., Rifai, M., Abouelmagd, K., Abo-Elnour, D. E., & Gamboa, L. L. (2025). Ketorolac as an analgesic in pediatric acute pain management: A systematic review and meta-analysis. Pediatric Emergency Care, 41(7), e34–e47.

Atefinezhad, M., Moghadamnia, A., Eftekhar, S. P., Moghadamnia, A. A., & Kazemi, S. (2022). Effect of Ketorolac on pharmacokinetics and pharmacodynamics of 5-fluorouracil: *In vivo* and *in vitro* study. Journal of Tropical Medicine, 2022(1), 5267861.

Avendaño, M. S., Martínez-Revelles, S., Aguado, A., Simões, M. R., González-Amor, M., Palacios, R., Guillem-Llobat, P., Vassallo, D. V, Vila, L., García-Puig, J., Beltrán, L. M., Alonso, M. J., Cachofeiro, M. V, Salaices, M., & Briones, A. M. (2016). Role of COX-2-derived PGE2 on vascular stiffness and function in hypertension. British Journal of Pharmacology, 173(9), 1541–1555.

Babuin, L., & Jaffe, A. S. (2005). Troponin: The biomarker of choice for the detection of cardiac injury. Canadian Medical Association Journal, 173(10), 1191–1202.

Barachini, S., Ghelardoni, S., Varga, Z. V, Mehanna, R. A., Montt-Guevara, M. M., Ferdinandy, P., & Madonna, R. (2023). Antineoplastic drugs inducing cardiac and vascular toxicity – An update. Vascular Pharmacology, 153, 107223.

Boarescu, I., & Boarescu, P.-M. (2024). Drug-induced myocardial infarction: A review of pharmacological triggers and pathophysiological mechanisms. Journal of Cardiovascular Development and Disease, 11(12), 406.
Boric, K., Dosenovic, S., Jelicic Kadic, A., Batinic, M., Cavar, M., Urlic, M., Markovina, N., & Puljak, L. (2017). Interventions for postoperative pain in children: An overview of systematic reviews. Pediatric Anesthesia, 27(9), 893–904.
Bormann, T., Maus, R., Stolper, J., Jonigk, D., Welte, T., Gauldie, J., Kolb, M., & Maus, U. A. (2021). Role of the COX2-PGE2 axis in *S. pneumoniae*-induced exacerbation of experimental fibrosis. American Journal of Physiology – Lung Cellular and Molecular Physiology, 320(3), L377–L392.
Bosch, D. J., Nieuwenhuijs-Moeke, G. J., van Meurs, M., Abdulahad, W. H., & Struys, M. M. R. F. (2022). Immune modulatory effects of nonsteroidal anti-inflammatory drugs in the perioperative period and their consequence on postoperative outcome. Anesthesiology, 136(5), 843–860.
Carneiro, R. M. F. de M., Cunha, R. S. da, Souza, L. M. de A., & Groppo, F. (2014). Preemptive analgesia of dexamethasone as compared to ketorolac tromethamine in simple tooth extractions. Revista Dor, 15(2), 83–86.
Chen, Q., Wang, Q., Zhu, J., Xiao, Q., & Zhang, L. (2018). Reactive oxygen species: Key regulators in vascular health and diseases. British Journal of Pharmacology, 175(8), 1279–1292.
Cheng, H., Huang, H., Guo, Z., Chang, Y., & Li, Z. (2021). Role of prostaglandin $E_2$ in tissue repair and regeneration. Theranostics, 11(18), 8836–8854.
Claar, D., Hartert, T. V., & Peebles Jr., R. S. (2015). The role of prostaglandins in allergic lung inflammation and asthma. Expert Review of Respiratory Medicine, 9(1), 55–72.
das Dores Lopes, P., de Assis, N., de Araújo, N. F., Moreno, O. L. M., de Oliveira Santana Jorge, K. T., e Castor, M. G. M., Teixeira, M. M., Soriani, F. M., dos Santos Aggum Capettini, L., Bonaventura, D., & de Assis Cau, S. B. (2022). COX/iNOS dependence for angiotensin-II-induced endothelial dysfunction. Peptides, 157, 170863.
Dolanbay, T., Makav, M., Gul, H. F., & Karakurt, E. (2021). The effect of diclofenac sodium intoxication on the cardiovascular system in rats. The American Journal of Emergency Medicine, 46, 560–566.
Elbrønd, V. S., Thomsen, M. B., Isaksen, J. L., Lunde, E. D., Vincenti, S., Wang, T., Tranum-Jensen, J., & Calloe, K. (2023). Intramural Purkinje fibers facilitate rapid ventricular activation in the equine heart. Acta Physiologica, 237(3), e13925.
Esparza-Villalpando, V., Ortiz-Barroso, G., & Masuoka-Ito, D. (2024). Evidence-based safety profile of oral ketorolac in adults: Systematic review and meta-analysis. Pharmacology Research and Perspectives, 12(6), e70033.
Forestell, B., Sabbineni, M., Sharif, S., Chao, J., & Eltorki, M. (2023). Comparative effectiveness of Ketorolac dosing strategies for emergency department patients with acute pain. Annals of Emergency Medicine, 82(5), 615–623.
Gokul, A. J., Chandur, V. K., & Shabarya, A. R. (2023). Non-selective Cox inhibitor NSAID's induced nephropathy: A systematic review. International Journal in Pharmaceutical Sciences, 1(12), 433–440.
Guan, J., Feng, N., Yang, K., Abudouaini, H., & Liu, P. (2024). The efficacy and safety of Ketorolac for postoperative pain management in lumbar spine surgery: A meta-analysis of randomized controlled trials. Systematic Reviews, 13(1), 275.
Irmak, K., Tüten, N., Karaoglu, G., Madazli, R., Tüten, A., Malik, E., & Güralp, O. (2021). Evaluation of cord blood creatine kinase (CK), cardiac troponin T (cTnT), N-terminal-pro-B-type natriuretic peptide (NT-proBNP), and s100B levels in nonreassuring foetal heart rate. The Journal of Maternal-Fetal and Neonatal Medicine, 34(8), 1249–1254.
Isiordia-Espinoza, M. A., Alonso-Castro, Á. J., Serafín-Higuera, N., Castañeda-Santana, D. I., de la Rosa Coronado, M., & Bologna-Molina, R. E. (2022). Postoperative administration of Ketorolac compared to other drugs for pain control after third molar surgery: A meta-analysis of double-blind, randomized, clinical trials. British Journal of Clinical Pharmacology, 88(6), 2591–2604.
Katusic, Z. S., Santhanam, A. V., & He, T. (2012). Vascular effects of prostacyclin: Does activation of PPARδ play a role? Trends in Pharmacological Sciences, 33(10), 559–564.
Koohsari, M., Shaki, F., & Jahani, D. (2016). Protective effects of edaravone against methamphetamine-induced cardiotoxicity. Brazilian Archives of Biology and Technology, 59, e16160093.
Lefchak, B., Morgan, D., Finch, M., Madhok, M., & Raschka, M. (2024). Ketorolac dose ceiling effect for pediatric headache in the emergency department. The Journal of Pediatric Pharmacology and Therapeutics, 29(5), 494–500.
Lin, Y.-N., Ibrahim, A., Marbán, E., & Cingolani, E. (2021). Pathogenesis of arrhythmogenic cardiomyopathy: Role of inflammation. Basic Research in Cardiology, 116(1), 39.
Liu, N., Guan, Y., Zhou, C., Wang, Y., Ma, Z., & Yao, S. (2022). Pulmonary and systemic toxicity in a rat model of pulmonary alveolar proteinosis induced by indium-tin oxide nanoparticles. International Journal of Nanomedicine, 17, 713–731.
Lu, H., Lai, K., Lin, S., & Dang, G. (2025). Anaphylactic shock induced by intravenous ketorolac: A case report. Heliyon, 11(3), e42236.
Maher, T. M., Evans, I. C., Bottoms, S. E., Mercer, P. F., Thorley, A. J., Nicholson, A. G., Laurent, G. J., Tetley, T. D., Chambers, R. C., & McAnulty, R. J. (2010). Diminished prostaglandin $E_2$ contributes to the apoptosis paradox in idiopathic pulmonary fibrosis. American Journal of Respiratory and Critical Care Medicine, 182(1), 73–82.
McDonald, E., Winters, B., Nicholson, K., Shakked, R., Raikin, S., Pedowitz, D. I., & Daniel, J. N. (2018). Effect of postoperative Ketorolac administration on bone healing in ankle fracture surgery. Foot and Ankle International, 39(10), 1135–1140.
Miao, Y., Yang, Y., Li, X., Meng, L., Mao, J., Zhang, J., Gao, J., Yang, C., Gu, X., Zhou, H., & Zhang, Y. (2023). Imrecoxib attenuates bleomycin-induced pulmonary fibrosis in mice. Heliyon, 9(11), e20914.
Milutinović, A., & Zorc-Pleskovič, R. (2012). Glycogen accumulation in cardiomyocytes and cardiotoxic effects after 3NPA treatment. Bosnian Journal of Basic Medical Sciences, 12(1), 15–19.
Mohammad, N., Darweesh, O., & Merkhan, M. (2025). The impact of disease-modifying medications on the lipid profile of patients with ischemic heart disease. Georgian Medical News, 363, 175–178.
Moro, M. G., Sanchez, P. K. V., Gevert, M. V., Baller, E. M., Tostes, A. F., Lupepsa, A. C., Baglie, S., & Franco, G. C. N. (2016). Gastric and renal effects of COX-2 selective and non-selective NSAIDs in rats receiving low-dose aspirin therapy. Brazilian Oral Research, 30(1), e127.
Nguyen, B. L., Fishbein, M. C., Chen, L. S., Chen, P.-S., & Masroor, S. (2009). Histopathological substrate for chronic atrial fibrillation in humans. Heart Rhythm, 6(4), 454–460.
Obayes, A. K., Mutar, W. M., Ayub, R. H., & Mohammed, S. A. (2020). Histological study of the effect of isoxicam on ovary of albino mice mus musculus. Indian Journal of Forensic Medicine and Toxicology, 14(2), 520–525.
Okwakpam, F. N., Dokubo, A., Monanu, M. O., & Uahomo, P. O. (2023). Cardioprotective effects of apocynin and curcumin against Diclofenac-induced cardiotoxicity in male Wistar rats via inhibition of oxidative stress. Scholars International Journal of Biochemistry, 6(07), 86–98.
Pászti, B., Prorok, J., Magyar, T., Árpádffy-Lovas, T., Györe, B., Topál, L., Gazdag, P., Szlovák, J., Naveed, M., Jost, N., Nagy, N., Varró, A., Virág, L., & Koncz, I. (2021). Cardiac electrophysiological effects of ibuprofen in dog and rabbit ventricular preparations: Possible implication to enhanced proarrhythmic risk. Canadian Journal of Physiology and Pharmacology, 99(1), 102–109.
Probst, C. K., Montesi, S. B., Medoff, B. D., Shea, B. S., & Knipe, R. S. (2020). Vascular permeability in the fibrotic lung. European Respiratory Journal, 56(1), 1900100.
Ricciotti, E., Haines, P. G., Chai, W., & FitzGerald, G. A. (2024). Prostanoids in cardiac and vascular remodeling. Arteriosclerosis, Thrombosis, and Vascular Biology, 44(3), 558–583.
S, D. L., B, V. G., & Murali, V. (2024). From prescription to pollution: The ecological consequences of NSAIDs in aquatic ecosystems. Toxicology Reports, 13, 101775.
Severino, P., D'Amato, A., Prosperi, S., Fanisio, F., Birtolo, L. I., Costi, B., Netti, L., Chimenti, C., Lavalle, C., Maestrini, V., Mancone, M., & Fedele, F. (2021). Myocardial tissue characterization in heart failure with preserved ejection fraction: From histopathology and cardiac magnetic resonance findings to therapeutic targets. International Journal of Molecular Sciences, 22(14), 7650.
Shalabi, M., Mahran, A. H., & Elsewif, T. (2024). Effect of submucosal cryotherapy compared with steroids and NSAIDs injections on Substance P and interleukin 6 pulpal release in experimentally induced pulpal inflammation in rabbits. Journal of Applied Oral Science, 32, e20240017.
Sorodoc, V., Sirbu, O., Lionte, C., Haliga, R. E., Stoica, A., Ceasovschih, A., Petris, O. R., Constantin, M., Costache, I. I., Petris, A. O., Morariu, P. C., & Sorodoc, L. (2022). The value of troponin as a biomarker of chemotherapy-induced cardiotoxicity. Life, 12(8), 1183.
Szczuko, M., Kozioł, I., Kotlęga, D., Brodowski, J., & Drozd, A. (2021). The role of thromboxane in the course and treatment of ischemic stroke: Review. International Journal of Molecular Sciences, 22(21), 11644.
Tashiro, J., Rubio, G. A., Limper, A. H., Williams, K., Elliot, S. J., Ninou, I., Aidinis, V., Tzouvelekis, A., & Glassberg, M. K. (2017). Exploring animal models that resemble idiopathic pulmonary fibrosis. Frontiers in Medicine, 4, 118.
Tejado, B. S. M., & Jou, C. (2018). Histopathology in HCM. Global Cardiology Science and Practice, 2018(3), 20.
Tjenggal, K. A., Sinuraya, R. K., Rahayu, C., & Abdulah, R. (2021). NSAID-induced adverse drug reaction: Mechanism and management. Indian Journal of Forensic Medicine and Toxicology, 15(2), 207.

Uddin, M. B., Hossain, A. M., Alam, M. M., & Hossain, A. S. (2008). Ketorolac and pethidine in post-operative pain relief. Bangladesh Journal of Pharmacology, 2(1), 498.
Van-Seuningen, I., & Davril, M. (1992). A rapid periodic acid-Schiff staining procedure for the detection of glycoproteins using the phastsystem. Electrophoresis, 13(1), 97–99.
Vupputuri, A., Sekhar, S., Krishnan, S., Venugopal, K., & Natarajan, K. U. (2015). Heart-type fatty acid-binding protein (H-FABP) as an early diagnostic biomarker in patients with acute chest pain. Indian Heart Journal, 67(6), 538–542.
Wang, Y., Wang, M., Samuel, C. S., & Widdop, R. E. (2022). Preclinical rodent models of cardiac fibrosis. British Journal of Pharmacology, 179(5), 882–899.
Zahkouk, S. A., El-Gendy, A. M., Eid, F. A., El-Tahway, N. A., & El-Shamy, S. A. (2015). Physiological and histological studies on the heart of male albino rats exposed to electromagnetic field and the protective role of silymarin and/or vitamin E. The Egyptian Journal of Hospital Medicine, 58, 94–108.
Zhou, X., Wang, Z., Wang, Y., Xu, G., Luo, M., Zhang, M., & Li, Y. (2025). Rutin ameliorates LPS-induced acute lung injury in mice by inhibiting the cGAS-STING-NLRP3 signaling pathway. Frontiers in Pharmacology, 16, 1590096.